

# Integrating Deep-Learning-Based Image Completion and Motion Planning to Expedite Indoor Mapping

Shmuel Y. Hayoun<sup>1</sup>, Elchanan Zwecher<sup>2</sup>, Eran Iceland<sup>3</sup>, Ahavatya Revivo<sup>4</sup>, Sean R. Levy<sup>5</sup>, and Ariel Barel<sup>6</sup>

**Abstract**—The challenge of autonomous indoor mapping is addressed. The goal is to minimize the time required to achieve a predefined percentage of coverage with some desired level of certainty. The use of a pre-trained generative deep neural network, acting as a map predictor, in both the motion planning and the map construction is proposed in order to expedite the mapping process. The issue of planning under partial observability is tackled by maintaining a belief map of the floorplan, generated by a deep neural network. This allows the agent to shorten the mapping duration, as well as enabling it to make better-informed decisions. This method is examined in combination with several motion planners for two distinct floorplan datasets. Simulations are run for several configurations of the integrated map predictor, the results of which reveal that by utilizing the prediction a significant reduction in mapping time is possible. When the prediction is integrated in both motion planning and map construction processes it is shown that the mapping time may in some cases be cut by over 50%.

## I. INTRODUCTION

Autonomous indoor mapping continues to be a relevant and challenging problem in many aspects, including the issue of motion planning. One of the main difficulties lies in the fact that the environment in which the mapping agent is intended to navigate is not known a priori. When considering practical constraints on the mapping agent's energetic capacity, it is desirable for the agent to determine a strategy that minimizes the mapping time. Unlike other optimally-solved path planning problems where the domain is fully observable from the start (e.g. shortest path problem), in this setting the agent equipped with on-board sensors (e.g. LIDAR, acoustic, stereo vision, etc.) accumulates partial and often noisy information only about its immediate surroundings. In this case, the derivation of an online, globally optimal solution may be impossible.

The problem of controlling autonomous agents in an unknown environment is invariably considered as a partially observable Markov decision process (POMDP), a popular

framework for representing sequential decision problems in which the state transitions with some uncertainty. In a POMDP an agent is tasked with sequential decision making based on partial observations of the state, with the objective of maximizing the expectation of some reward which is a function of the state and action. Each action performed by the agent causes the state to change stochastically based only on the current state and action. Since it cannot directly observe the state, the agent's decisions are based solely on observations that are stochastically generated by the state itself.

Consider the problem of indoor mapping where the objective is to minimize the time to reach a predefined minimal level of confidence across some required portion of the map. A naïve approach would be to construct the map based exclusively on the observations. However, if the floorplan to be mapped possesses certain attributes which can be learned and generalized, observing the entire map is no longer necessary. Within the POMDP framework the state in the mapping problem can be represented by the partially observed map. Now the motion planning problem can either be solved heuristically at each time step using belief space planning (BSP) or as part of the initial POMDP. In the former case the agent's trajectory is planned while maintaining a belief map and regarding it as the fully observed state. In the latter one might consider the use of reinforcement learning to handle the motion planning.

This paper presents the proposed methodology of integrating a trained image completion network with both the motion planning and map construction procedures in order to expedite indoor exploration. The issue of planning under partial observability is tackled by maintaining a belief map of the floorplan, generated by a deep neural network. This allows the agent to shorten the mapping duration, as well as enabling it to make better-informed decisions.

## II. RELATED WORK

In past works mapping by predictions based on partial observations was achieved by extracting geometric features representing the regularities of the indoor environment, as presented in [1], [2]. However, in recent years neural networks have outperformed many traditional methods in estimation, classification and prediction. Among other things, they show impressive results in the realm of data generation and image restoration, also known as inpainting [3]–[5]. They have also been used to recover partial 2D maps [6]–[11]. However, most of the work on image restoration is concerned with denoising or "natural-looking" data

<sup>1</sup>Shmuel Y. Hayoun is with the Faculty of Aerospace Engineering, Technion - Israel Institute of Technology, Haifa, Israel [shmuli.hayoun@gmail.com](mailto:shmuli.hayoun@gmail.com)

<sup>2</sup>Elchanan Zwecher is with the Computer Science Department, Hebrew University of Jerusalem, Jerusalem, Israel [elchanan4567@gmail.com](mailto:elchanan4567@gmail.com)

<sup>3</sup>Eran Iceland is with the Computer Science Department, Hebrew University of Jerusalem, Jerusalem, Israel [eran.iceland@gmail.com](mailto:eran.iceland@gmail.com)

<sup>4</sup>Ahavatya Revivo is with the Computer Science Department, Bar-Ilan University, Ramat Gan, Israel [ahavatya@gmail.com](mailto:ahavatya@gmail.com)

<sup>5</sup>Sean R. Levy is with the Aerospace Engineering Department, Technion, Haifa, Israel [sean2102@gmail.com](mailto:sean2102@gmail.com)

<sup>6</sup>Ariel Barel is an academic visitor at the Computer Science Department, Technion - Israel Institute of Technology, Haifa, Israel [arielba@technion.ac.il](mailto:arielba@technion.ac.il)

generation, in the sense that since the exact missing or blurred observation cannot be obtained, a replacement to the unknown image that is as "natural" as possible is sought [12], [13]. Regarding 2D map completion, most previous work is concentrated on semantic classification [7], [8] and not in a pixel-by-pixel mapping. Moreover, invariably the entire image is used in order to map only a local missed patch of it [2], [11], [14]. Another works on navigation over 2D maps, looks for an optimal local information gain actions [15], local matching topologies [16], navigating using reinforcement learning techniques [17], [18], or exploiting existing plans of the building [19]. Conversely, in the present work a prediction of the complete image is performed, given relatively few observations. These differences also affect the choice of the type of neural network architecture.

### III. PROBLEM FORMULATION

Consider the problem of mapping a bounded indoor environment by an autonomous agent equipped with range sensors. The environment topology is assumed to possess some features common with an available dataset of floorplans. Since the present work is focused on the issue of motion planning, the problem is simplified by assuming that the localization problem is solved and neglecting any measurement noise. The desired constructed map, the boundary of which is known a priori, is given in the form of a 2D binary occupancy grid in which each cell may be either vacant or occupied. The agent's objective is to minimize the time to reach a predefined percentage of coverage with some desired level of certainty.

### IV. PROPOSED SOLUTION

Any basic mapping system design includes a map constructor which is generally fed sensory inputs and a motion planner which bases its decision making upon the existing constructed map. Normally, the constructed map simply includes the accumulated observations.

The proposed solution consists of enhancing the performance of the motion planning and map construction processes through the incorporation of learned experience. Concretely, the proffered mapping system includes a deep artificial image completing neural network, trained in a supervised manner on numerous examples of partial observation maps to output a prediction over the entire indoor environment. The mapping system in its entirety is depicted in Fig. 1. The map constructor now receives the map prediction in addition to the accumulated observations, and produces a combined occupancy grid composed of the observations and the prediction in unobserved areas.

As discussed earlier, experience-based motion planning has been proven to expedite the mapping process. Therefore, expected potential benefits include savings in observations (measurements) required for reaching the desired mapping goal as well as improved, more informed decision making on the motion planner's part.

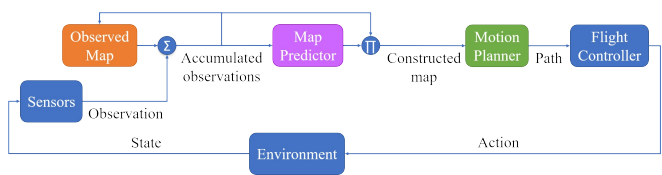


Fig. 1. Proposed mapping system. The  $\Sigma$  symbol represents the observations accumulation operator. The  $\Pi$  symbol represents the observations and prediction combination operator

### V. MAP PREDICTION

The map predictor is a deep neural network tasked with recovering the entire structural map from given partial observations. Essentially, the predictor is a function that takes a partially observed occupancy grid as an input and outputs a probability distribution over the same grid. The prediction over each cell is the probability of it being occupied (part of a wall). The output is expected to preserve the given observations, i.e. to output the already observed pixels as they are with very high probability. In order to get a categorized probable map after obtaining a prediction from the network a thresholding is performed in the following manner over each cell  $m_i$  in the occupancy grid:

$$m_i = \begin{cases} \text{Occupied,} & \text{if } p_i > \frac{1+\tau_c}{2} \\ \text{Vacant,} & \text{if } p_i < \frac{1-\tau_c}{2} \\ \text{Unknown,} & \text{otherwise} \end{cases}, \quad (1)$$

where  $p$  is the probability of wall and  $\tau_c \in [0,1]$  is the threshold corresponding to category  $c$  ( $\tau_c$  can also be considered the confidence level of category  $c$ ). Unlike other similar works in which both thresholds are trivially set to 0.5, the "unknown" category was added since it was perceived that in areas where very few observations exist obtaining a reliable distinct prediction is practically impossible. The probability of any cell, situated far away from any observations, being occupied will quite likely tend towards the general probability of any random cell being occupied, which is simply the ratio of occupied cells (walls) in the structure. This value is of course expected to be significantly less than 0.5. Therefore, the "unknown" category is intended to reflect when the prediction is unreliable.

#### A. Architecture

The map predictor, illustrated in Fig. 2, is a classifying network, implemented as a convolutional autoencoder with symmetric skip connections. As discussed above, image completion is frequently accomplished using data generation methods, such as generative adversarial networks (GANs) [20] or variational autoencoders (VAEs) [21] to produce "natural-looking" images. However, since in the present case an exact reconstruction of the floorplan is coveted, simply generating "natural-looking" maps is insufficient.

The network receives as input a three channel image where each channel corresponds to one of three categories: occupied, vacant or unknown. Each cell in the occupancy grid is represented by a triplet corresponding to these three

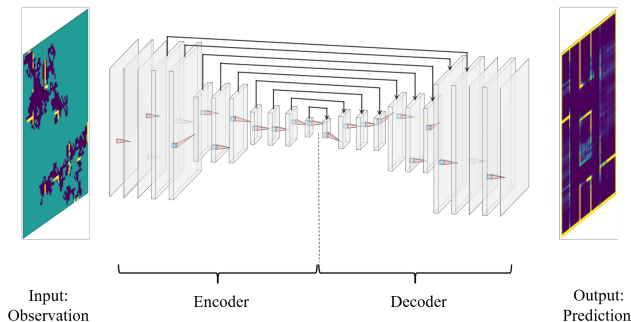


Fig. 2. Map predictor architecture – ResNet-styled convolutional autoencoder

categories, such that only one of them equals 1 while the two others are 0, also known as a one-hot encoding. The generated output is of the same dimensions as the input.

The core of the architecture is comprised of nine encoding layers and nine decoding layers. Each encoding layer contains  $25\ 3 \times 3$ -sized kernels. Every third layer also includes a stride of 2 in order to obtain a reduced sized encoded representation of the input in the so-called latent space. Similarly, in an inverse manner, every third layer in the decoder incorporates 3D transposed convolution with a stride 2 in order to recover original map size. The addition of the symmetric skip-connection, which was reported by [3] to improve performance, is used not in order to enrich the hypothesis class (as done for more elaborate architectures), but mostly in order to improve the optimization process by aiding the back-propagation algorithm in overcoming the exploding/vanishing gradient problem [22]. Moreover, in the present case there one might also see the sense in repeatedly "reminding" the subsequent layers in the network of the output from previous layers, since the observations should be regarded while estimating the unknown cells.

Two more dominant features were added to the network. The first was introducing an initial hidden layer tasked with augmenting the input so as to improve the optimization process. The added first layer is a convolution layer with a single  $1 \times 1 \times 3$  kernel without bias that takes the three-channeled input and outputs a single channel image which now contains in each cell one of three learned optimal values representing the three possible categories. This new representation of the input enhances the network optimization during training. The second feature was stacking the input observation on to the input to the last hidden layer, such that the number of channels of that layer is increased by one. This operation, similar to the skip connection, serves as a "reminder" of the input immediately prior to the final map reconstruction stage. This is done with the intent of accentuating the observations in order to improve the quality of the reconstructed output.

### B. Optimization

The neural net (before thresholding) is designed to output a probability map which the result of extensive training, during

which the following optimization criteria is to be minimized:

$$\mathcal{L} = - \sum_{i \in \mathcal{I}} [y_i \log(p_i) + (1 - y_i) \log(1 - p_i)]. \quad (2)$$

$y_i$  is the actual label of pixel  $i$ , i.e. 0 if vacant and 1 if occupied and, accordingly,  $p_i$  is the probability of  $i$  being occupied. The chosen function  $\mathcal{L}(\cdot)$ , otherwise known as the loss function, is the binary cross entropy loss - a commonly used loss function for classification problems. This function measures the Kullback–Leibler divergence between the true distribution (i.e. label) and the predicted distribution over a pixel.

### C. Training Sets

The map predictor was trained on two distinct datasets, differing mainly in level of variance of the building layouts' geometrical features, as listed in TABLE I. Several examples from each dataset are displayed in Fig. 3. Fig. 4 exhibits the distributions of the buildings' fraction of walls in each dataset, illustrating their structural differences.

TABLE I  
DATASETS CHARACTERISTICS

		<i>Datasets</i>		
		$\mathcal{D}_1$	$\mathcal{D}_2$	
<i>Characteristics</i>	Source	Independently generated	HouseExpo [14]	
	Size	50,000	35,126	
	Contour	Identical Convex (rectangle)	Varying Convex & concave	
	Variance	Size	Low	High
		%Walls	Low	High
		Topology	Low	High

A simplified simulation was created for accumulating a variety of observations in a given map. In a given run the observations were obtained by selecting an initial location within the empty occupancy grid at random and accumulating observations randomly in a tree-like fashion to a certain depth which was random as well. The simulation was run 5 times on each floorplan in each dataset. The collected

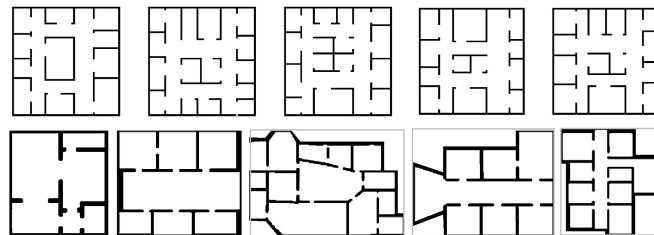


Fig. 3. Illustrative floorplan examples. The top row includes examples from  $\mathcal{D}_1$  and the bottom row includes examples from  $\mathcal{D}_2$

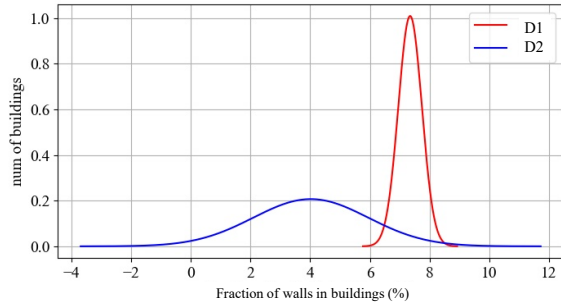


Fig. 4. Fraction of walls distribution for the different datasets

observations in each dataset constituted the training set for the corresponding network.

#### D. Evaluation

1) *Evaluation Index*: A plausible characteristic of the presented mapping problem is the possibility of there being a substantial difference between the overall percentages of occupied and vacant spaces. Accordingly, the chosen performance indicator is the  $F_1$  score, an accepted key index for testing the quality of a binary classifier over imbalanced data. This metric incorporates two measures with respect to the minority class – in this case the *occupied/wall* class – namely the precision and sensitivity/recall. The precision equals the percentage of actual walls out of the total of classified walls while the recall constitutes the percentage of correctly classified walls out of the total of actual walls. The  $F_1$  score is the harmonic mean of the two. Following the probabilistic view, by which the *occupied/wall* class can be considered as *true* and the *vacant* class as *false*,

$$\begin{aligned} \text{precision} &= \frac{TP}{TP + FP} \\ \text{recall} &= \frac{TP}{TP + FN} \end{aligned} ,$$

where  $TP$  is the total of true positives,  $FP$  is the total of false positives and  $FN$  is the total of false negatives. The  $F_1$  score can be expressed using these terms, yielding

$$F_1 = 2 \cdot \frac{\text{precision} \cdot \text{recall}}{\text{precision} + \text{recall}} = \frac{2TP}{2TP + FN + FP}. \quad (3)$$

Employing this evaluation index the map predictor's performance was gauged.

2) *Test Results*: Three identically structured networks (as outlined in Section V-A) were trained separately on  $\mathcal{D}_1$  and  $\mathcal{D}_2$ , one for each dataset. The performance of each network was measured across 30 floorplans from its corresponding dataset in terms of the  $F_1$  scores. The baseline for comparison is the scores of the observations themselves.

Fig. 5 portrays the  $F_1$  scores as a function of the number of observations. A significant improvement can be discerned in the performance obtained by the map predictor.

## VI. MOTION PLANNING

This section includes an outline of the different motion planning algorithms that were considered.

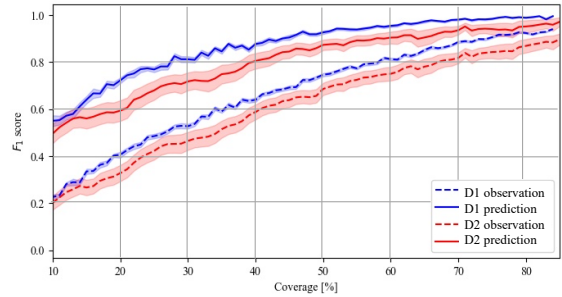


Fig. 5. Prediction  $F_1$  scores over the different datasets

#### A. Problem Formulation

The occupancy grid is regarded as an undirected weighted graph, in which the nodes are the vacant cells and the vertices represent the contiguity of any two neighbouring nodes. The weight of each vertex is equal to the euclidean distance between the centers of its corresponding adjacent cells.

The agent's objective is to find a path along the graph which minimizes the time to expose a desired portion of the same graph with some minimum level of certainty.

#### B. Motion Planning Algorithms

The partial observability of the graph which is to be explored eliminates the possibility of finding an optimal route. Therefore, heuristic-driven motion planners, which strive to maximize some instantaneous utility, were examined [23], [24]. This utility, while not a direct representation of the original objective, is nonetheless a reflection of it, albeit in a more immediate sense.

During the mapping process, apart from its current location, the agent bases its decided motion upon the accumulated observations, the map prediction, the constructed map, the visibility front, the map graph representation as well as some subset of the shortest distance paths in the graph.

Three path planning algorithms were considered, as detailed in the following.

1) *Random Exploration*: Follows the shortest path to a randomly chosen point on the visibility front.

2) *Greedy Selection*: Take a step along the shortest path to the point on the visibility front which yields the highest utility. The utility of a point on the visibility front  $v \in \mathcal{V}$  was chosen to be of the following form

$$\text{utility}(v) = \frac{\text{reward}(v)}{1 + \text{cost}(v)} \quad , \quad (4)$$

where  $\text{reward}(v)$  and  $\text{cost}(v)$  are the estimated reward and cost to arrive at  $v$ , respectively. Two variants (with respect to the definition of  $\text{utility}(\cdot)$ ) of this algorithm were considered, as follows.

**Nearest Frontier**, chooses the point on the visibility front with the minimal shortest distance path from the agent's current position. i.e.,

$$\begin{aligned} \text{reward}(v) &\equiv 1, \\ \text{cost}(v) &\triangleq \text{shortest distance to point } v. \end{aligned}$$

**Cost-Utility**, by which the most cost effective point (with maximal benefit-to-effort ratio) on the visibility front is selected. In this version

$reward(v) \triangleq$  potential confidence increase at point  $v$ ,

$cost(v) \triangleq$  shortest distance to point  $v$ .

## VII. SIMULATIONS

To assess the potential increase in performance from integrating the map predictor the aforementioned motion planning methods were examined in the following three prediction-based configurations: a) observation-based motion planning and map construction, b) observation-based motion planning and prediction-based map construction, c) prediction-based motion planning and map construction.

### A. Simulation Testbed

A simplified grid world simulation was set up in Python, in which the mapping agent, situated in a certain cell, is free to move to any of its eight neighbouring cells, provided they are vacant. The agent is equipped with 16 fixed on-board range sensors arranged in equal angular intervals of  $22.5^\circ$  with an effective range of 20 pixels.

### B. Simulation Results & Analysis

The summarized mapping performance is presented in Fig. 6 – Fig. 8. The results were obtained from simulation runs over 30 maps in each dataset. The evident advantage of integrating the map predictor in both the map construction and the motion planning processes is discussed below.

An example run of the *Cost-Utility* motion planner using prediction-based planning and map construction on a sample map from  $\mathcal{D}_1$  is included in Fig. 6. A comparison between the observations maps (leftmost column) and constructed maps (second column from the right) illustrates the substantial advantage of including the prediction in the map construction process. As demonstrated here, for marginal errors the map predictor holds the capacity to nearly double the map exposure for the final set of observations.

Fig. 7 and Fig. 8 include statistical performance data, accumulated over 30 floorplans from each dataset. The performance, measured in terms of the mapping duration, is normalized in each floorplan with respect to its size in order for the results across different-sized maps to be comparable.

Fig. 7 shows the mapping duration statistics for the three prediction-based configurations. The distinct advantage of using the map predictor to construct the output map is again evident, yielding a reduction of up to 40% for  $\mathcal{D}_1$  and 60% for  $\mathcal{D}_2$  on average in mapping time, as obtained for *Cost-Utility*. When the map predictor is incorporated into the motion planning process as well, the estimated savings in mapping time increases to roughly 52% for  $\mathcal{D}_1$  and 67% for  $\mathcal{D}_2$  on average. the mapping duration errors, corresponding to the results in the previous figure are given. Note that for a required percentage of mapping of 98% the inherent nominal error should be 2%. Though compared to observation-based mapping the map predictor on average adds errors to the constructed map, they are negligible (less than 0.1%). On

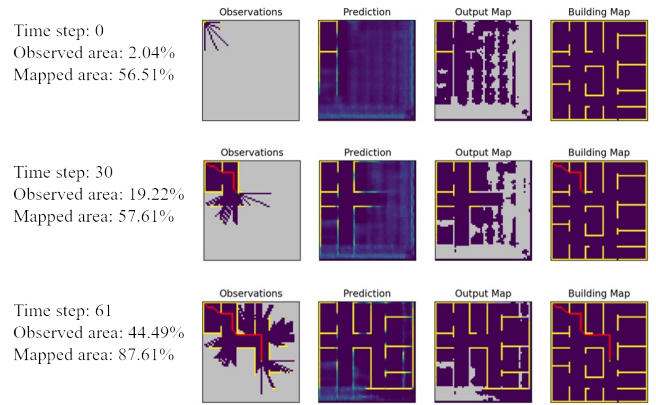


Fig. 6. Example prediction-based path for *Cost-Utility* over a single floorplan from  $\mathcal{D}_1$  for a required 85% coverage at an 85% level of confidence for both classification thresholds. The depicted outcome for each planner include the observations map (leftmost), the map prediction (second from the left), the constructed map (second from the right) and the ground truth map (rightmost). The observations and ground truth maps include the agent's location (green) and its traversed path (red). Vacant, occupied and unknown cells in each map are indicated in deep purple, yellow and grey, respectively

the other hand, it can be seen that the map predictor is also capable of supplying a higher percentage of exposure for the same coverage requirement.

Fig. 8 shows the mapping performance of the prediction-based planning and map construction configuration for different values of the required exposed portion of the map over  $\mathcal{D}_1$  and  $\mathcal{D}_2$ .

## VIII. FUTURE WORK

In future work the authors plan to examine reinforcement learning as a solution to the presented mapping problem. The first aspect to consider will be whether to train a substitute motion planner to operate alongside the map predictor or whether to replace both the map predictor and the motion planner with a single model as an end-to-end solution. An additional aim is to extend the current problem to one in which aside from never having seen the environment that is to be explored the agent will have no prior knowledge as to the building's affiliation to a specific dataset. The initial approach will be to train a preliminary classifying network to determine the building's most probable denomination, according to which the appropriate map predictor will be employed.

## IX. CONCLUSIONS

The problem of autonomous indoor mapping in which the goal is to minimize the time to obtain a required percentage of coverage with a wanted level of certainty was considered. The proposed method by which to expedite the mapping process consisted of integrating a map predictor, realized as a pre-trained generative deep neural network, in both the motion planning and the map construction.

Two distinct datasets of floorplans were examined, differing in several key aspects of the topology of the structures in each set. Two respective "specialized" map predictors

		Configuration					
		No prediction		Prediction-based map		Prediction-based map and planning	
		D1	D2	D1	D2	D1	D2
Mapping Duration	Augmented Random Walk	112.333 (5.391)	85.115 (33.136)	83.864 (25.813)	54.619 (28.078)	43.601 (15.859)	43.266 (28.588)
	Nearest Frontier	85.672 (8.826)	67.603 (19.814)	61.777 (14.443)	44.833 (28.953)	35.387 (3.653)	35.218 (24.314)
	Cost - Utility	73.752 (11.016)	62.011 (21.775)	38.961 (13.142)	26.742 (62.011)	27.089 (5.240)	24.404 (43.113)
Mapping Accuracy	Augmented Random Walk			0.995 (0.011)	0.996 (0.016)	1 (0)	0.994 (0.024)
	Nearest Frontier			1 (0)	0.999 (0.002)	1 (0)	0.999 (0.003)
	Cost - Utility			0.999 (0.001)	0.999 (0.002)	0.999 (0.001)	0.999 (0.003)
FI Score	Augmented Random Walk			0.949 (0.101)	0.958 (0.113)	0.9991 (0.008)	0.941 (0.138)
	Nearest Frontier			0.994 (0.006)	0.978 (0)	0.991 (0.006)	0.962 (0.072)
	Cost - Utility			0.987 (0.012)	0.038 (0)	0.983 (0.008)	0.967 (0.066)

Fig. 7. Mapping duration statistics of the different motion planners in three prediction-based configurations over the different datasets. The results were obtained for a required coverage of 98% and the classification confidence thresholds set to 95% for occupancy and 93% for vacancy

were produced - each trained separately on a different dataset. The obtained map predictors were each examined in combination with several motion planners: a simple random exploration and two variations of a greedy search, namely *nearest frontier* and *cost-utility* planners. The prediction-based motion planning methodology serves as a belief space planning realization, whereby the action at each time step is planned based on the predicted map, which is considered to be true.

Simulations were run on representative groups of floorplans from each dataset. The proposed configuration of the fully integrated map predictor was compared to that of observation-based motion planning and map construction and to an observation-based motion planning followed by prediction-based map construction setup. The results highlighted the significant potential improvement in terms of mapping time when incorporating the prediction in both the motion planning and the map construction processes. Furthermore, a comparison between the different motion planners revealed that without further insight simple random exploration can potentially at times outperform more sophisticated planners. Of the examined planners *cost-utility*'s performance surpassed the others'. Finally, an analysis of the affect of the hyperparameters' values on the obtained mapping times and resulting errors was carried out, illustrating the manner by which a user would be able to choose appropriate values in order to obtain a desired amount of coverage at a required confidence level within a given time limit.

		Desired Coverage [%] n					
		85		90		98	
		D1	D2	D1	D2	D1	D2
Mapping Duration	Augmented Random Walk	27.637 (9.638)	17.073 (16.238)	32.523 (11.839)	22.345 (19.949)	43.601 (15.859)	43.266 (28.588)
	Nearest Frontier	22.492 (3.077)	14.215 (7.757)	26.415 (2.605)	18.684 (10.066)	35.387 (3.653)	35.218 (24.314)
	Cost - Utility	15.592 (2.758)	11.223 (6.356)	17.713 (3.718)	14.099 (6.489)	27.089 (5.240)	24.404 (43.113)
Mapping Accuracy	Augmented Random Walk	0.999 (0.001)	0.999 (0.002)	1 (0)	0.998 (0.007)	1 (0)	0.994 (0.024)
	Nearest Frontier	1 (0)	0.998 (0.003)	1 (0)	0.999 (0.003)	1 (0)	0.999 (0.003)
	Cost - Utility	1 (0)	0.999 (0.002)	1 (0)	0.998 (0.004)	0.999 (0.001)	0.999 (0.003)
FI Score	Augmented Random Walk	0.989 (0.010)	0.893 (0.132)	0.985 (0.011)	0.900 (0.141)	0.9991 (0.008)	0.941 (0.138)
	Nearest Frontier	0.986 (0.009)	0.889 (0.137)	0.984 (0.011)	0.902 (0.132)	0.991 (0.006)	0.962 (0.072)
	Cost - Utility	0.980 (0.013)	0.895 (0.121)	0.981 (0.014)	0.906 (0.120)	0.983 (0.008)	...0.967 (0.066)

Fig. 8. Mapping duration statistics of the different motion planners in the prediction-based planning and map construction configuration over  $\mathcal{D}_1$  and  $\mathcal{D}_2$ . The results were obtained for the classification confidence thresholds set to 95% for occupancy and 93% for vacancy

## REFERENCES

- [1] M. Luperto, L. Fochetta, and F. Amigoni, "Exploration of indoor environments predicting the layout of partially observed rooms," *arXiv preprint arXiv:2004.06967*, 2020.
- [2] J. M. Pimentel, M. S. Alvim, M. F. Campos, and D. G. Macharet, "Information-driven rapidly-exploring random tree for efficient environment exploration," *Journal of Intelligent & Robotic Systems*, vol. 91, no. 2, pp. 313–331, 2018.
- [3] X.-J. Mao, C. Shen, and Y.-B. Yang, "Image restoration using convolutional auto-encoders with symmetric skip connections," *arXiv preprint arXiv:1606.08921*, 2016.
- [4] G. Liu, F. A. Reda, K. J. Shih, T.-C. Wang, A. Tao, and B. Catanzaro, "Image inpainting for irregular holes using partial convolutions," in *Proceedings of the European Conference on Computer Vision (ECCV)*, 2018, pp. 85–100.
- [5] J. Yu, Z. Lin, J. Yang, X. Shen, X. Lu, and T. S. Huang, "Free-form image inpainting with gated convolution," in *Proceedings of the IEEE International Conference on Computer Vision*, 2019, pp. 4471–4480.
- [6] O. Asraf and V. Indelman, "Experience-based prediction of unknown environments for enhanced belief space planning," in *2020 IEEE/RSJ International Conference on Intelligent Robots and Systems (IROS)*, 2020.
- [7] A. Pronobis and R. P. Rao, "Learning deep generative spatial models for mobile robots," in *2017 IEEE/RSJ International Conference on Intelligent Robots and Systems (IROS)*. IEEE, 2017, pp. 755–762.
- [8] W. Qi, R. T. Mullanpudi, S. Gupta, and D. Ramanan, "Learning to move with affordance maps," *arXiv preprint arXiv:2001.02364*, 2020.
- [9] J. A. Caley, N. R. Lawrance, and G. A. Hollinger, "Deep learning of structured environments for robot search," *Autonomous Robots*, vol. 43, no. 7, pp. 1695–1714, 2019.
- [10] K. Katyal, K. Popek, C. Paxton, P. Burlina, and G. D. Hager, "Uncertainty-aware occupancy map prediction using generative networks for robot navigation," in *2019 International Conference on Robotics and Automation (ICRA)*. IEEE, 2019, pp. 5453–5459.
- [11] R. Shrestha, F.-P. Tian, W. Feng, P. Tan, and R. Vaughan, "Learned map prediction for enhanced mobile robot exploration," in *2019 International Conference on Robotics and Automation (ICRA)*. IEEE, 2019, pp. 1197–1204.
- [12] S. Iizuka, E. Simo-Serra, and H. Ishikawa, "Globally and locally

- consistent image completion,” *ACM Transactions on Graphics (ToG)*, vol. 36, no. 4, pp. 1–14, 2017.
- [13] J. Yu, Z. Lin, J. Yang, X. Shen, X. Lu, and T. S. Huang, “Generative image inpainting with contextual attention,” in *Proceedings of the IEEE conference on computer vision and pattern recognition*, 2018, pp. 5505–5514.
- [14] T. Li, D. Ho, C. Li, D. Zhu, C. Wang, and M. Q.-H. Meng, “Housexpo: A large-scale 2d indoor layout dataset for learning-based algorithms on mobile robots,” *arXiv preprint arXiv:1903.09845*, 2019.
- [15] S. Bai, F. Chen, and B. Englot, “Toward autonomous mapping and exploration for mobile robots through deep supervised learning,” in *2017 IEEE/RSJ International Conference on Intelligent Robots and Systems (IROS)*. IEEE, 2017, pp. 2379–2384.
- [16] M. Saroya, G. Best, and G. A. Hollinger, “Online exploration of tunnel networks leveraging topological cnn-based world predictions,” in *Proc. of IEEE/RSJ IROS*, 2020.
- [17] L. Tai and M. Liu, “A robot exploration strategy based on q-learning network,” in *2016 IEEE International Conference on Real-time Computing and Robotics (RCAR)*. IEEE, 2016, pp. 57–62.
- [18] F. Niroui, K. Zhang, Z. Kashino, and G. Nejat, “Deep reinforcement learning robot for search and rescue applications: Exploration in unknown cluttered environments,” *IEEE Robotics and Automation Letters*, vol. 4, no. 2, pp. 610–617, 2019.
- [19] M. Luperto, D. Fusi, N. A. Borghese, and F. Amigoni, “Robot exploration using knowledge of inaccurate floor plans,” in *2019 European Conference on Mobile Robots (ECMR)*. IEEE, 2019, pp. 1–7.
- [20] I. Goodfellow, J. Pouget-Abadie, M. Mirza, B. Xu, D. Warde-Farley, S. Ozair, A. Courville, and Y. Bengio, “Generative adversarial nets,” in *Advances in neural information processing systems*, 2014, pp. 2672–2680.
- [21] I. Higgins, L. Matthey, X. Glorot, A. Pal, B. Uria, C. Blundell, S. Mohamed, and A. Lerchner, “Early visual concept learning with unsupervised deep learning,” *arXiv preprint arXiv:1606.05579*, 2016.
- [22] K. He, X. Zhang, S. Ren, and J. Sun, “Deep residual learning for image recognition,” *ComputerScience*, 2015.
- [23] B. Yamauchi, “A frontier-based approach for autonomous exploration,” in *Proceedings 1997 IEEE International Symposium on Computational Intelligence in Robotics and Automation CIRA'97: Towards New Computational Principles for Robotics and Automation*. IEEE, 1997, pp. 146–151.
- [24] S. Wirth and J. Pellenz, “Exploration transform: A stable exploring algorithm for robots in rescue environments,” in *2007 IEEE International Workshop on Safety, Security and Automation Robotics*. IEEE, 2007, pp. 1–5.